Clean Version

OPTIMIZATION OF TORREFACTION CONDITIONS OF COFFEE INDUSTRY RESIDUES USING DESIRABILITY FUNCTION APPROACH

C. Buratti[a], M. Barbanera[a], E. Lascaro[a], F. Cotana[a]
[a] CRB - Biomass Research Centre, Via G. Duranti, 63, 06125 Perugia, Italy

Abstract

The aim of the present study is to analyze the influence of independent process variables such as temperature, residence time, and heating rate on the torrefaction process of coffee chaff (CC) and spent coffee grounds (SCGs). Response surface methodology and a three-factor and three-level Box-Behnken design were used in order to evaluate the effects of the process variables on the weight loss (W_L) and the Higher Heating Value (HHV) of the torrefied materials. Results showed that the effects of the three factors on both responses were sequenced as follows: temperature > residence time > heating rate. Data obtained from the experiments were analyzed by analysis of variance (ANOVA) and fitted to second-order polynomial models by using multiple regression analysis. Predictive models were determined, able to obtain satisfactory fittings of the experimental data, with coefficient of determination (R^2) values higher than 0.95.
An optimization study using Derringer's desired function methodology was also carried out and the optimal torrefaction conditions were found: temperature 271.7°C, residence time 20 min, heating rate 5°C/min for CC and 256.0°C, 20 min, 25°C/min for SCGs. The experimental values closely agree with the corresponding predicted values.

Keywords: Torrefaction, Coffee residue, Response surface methodology; Desirability function; Optimization

1. Introduction

Torrefaction is a thermal pretreatment process operating at low temperature (200-300°C), under atmospheric conditions, in the absence of oxygen. It is interesting for upgrading ligno-cellulosic biomass to a higher quality fuel, and for its following conversion into heat or other energy carriers, such as electricity and biofuels (Poudel et al., 2015). During torrefaction, the bound and unbound moisture as well as high volatile fraction of organic components, particularly hemicellulose and some lignin, are released from biomass. They form a solid product mainly composed of cellulose and lignin (Medic et al., 2012), with lower H/C and O/C ratios and higher carbon content than raw material (Lee et al., 2012). However, the thermal decomposition behaviour of each kind of biomass can greatly vary with of the polymer structure and the ash content, that may catalyze some reactions (Lee et al., 2012).
The kinetic mechanism of the torrefaction is also influenced by the operating parameters, such as the reaction temperature, the residence time, and the heating rate (Mundike et al, 2016). Many researchers showed that the torrefaction temperature is the determining factor for obtaining the most optimized yield and quality of the final solid product (Phanphanich and Mani, 2011; Chen and Kuo, 2011; Medic et al., 2012). In general, the higher the torrefaction temperature, the more oxygenated compounds are converted into volatiles, obtaining a char-like solid product characterized by higher energy density. The effect of the

residence time on the char yield and Higher Heating Value (HHV) is more difficult to interpret. Mundike et al. (2016) for Lantana camara plant, showed that increasing residence time from 25 to 80 min at 280 °C, char yield decreases from 65.97% to 52.42% and HHV increases from 22.37 MJ/kg to 24.95 MJ/kg. Chiou et al. (2015) investigated several pomaces and nut shells, and found that mass yields decrease with longer residence time along with the HHV values; in particular for apple pomace, the HHV value of char decreases from 26.1 MJ/kg to 23.0 MJ/kg by increasing residence time from 20 min to 60 min at 260°C. As regards the influence of the heating rate, only one study analyzes its effect on char yield and HHV (Mundike et al., 2016), highlighting a minimal influence of this operating parameter on the torrefaction process.

Data in the Literature show that operating parameters should not be analyzed individually and that it is necessary to employ statistical methods taking into account the interactions between parameters. One of the most widespread methodologies to test process parameters and their interactive effects is the Response Surface Methodology (RSM) (Myers et al., 2009). This multivariate statistic method consists of designing a mathematical model that can exactly describe the overall process, in order to achieve best system performance (Maran and Manikandan, 2012; Cotana et al., 2015). However, if the process requires the optimization of several responses, the independent evaluation of each response cannot be the right way to find the best solution for all responses concurrently because improving one response can worsen the other one (Costa et al., 2011). For these cases, desirability function can be employed to solve this conflict, finding an optimal experimental condition to successfully fulfill the optimization of all responses (Viacava et al., 2015).

Although in the Literature there are several studies that involved torrefaction of biomass from different raw materials (e.g. oil palm waste (Aziz et al., 2012), wheat straw (Shang et al., 2012)), there had been only one work (Chen et al., 2012) that focused on the torrefaction of coffee residues, evaluating the influence of the torrefaction conditions on its properties and structures, but not defining the optimal set of the operating parameters.

Coffee is the second largest traded product in the world and a huge quantity and variety of residues is generated during processing from fruit to cup (Murthy and Madhava Naidu, 2012). The International Coffee Organization (ICO, 2016) estimated that about 9 million tons of coffee bean was consumed in 2016, the majority of which in the EU, USA, Brazil, and Japan [ICO]. Coffee by-products are obtained from coffee production (e.g. husk, pulp, parchment, mucilage), roasting industries (e.g. coffee silverskin) and also during soluble coffee preparation (spent coffee grounds) (Cruz et al., 2014). Two interesting coffee residues for the char production are the parchment skin, often referred to a coffee chaff (CC), that is a thin layer of endocarp, yellowish in colour, inside the coffee beans, and the spent coffee grounds (SCGs), which are mainly obtained from large facilities that process coffee bean to produce soluble coffee. CC represents about 4.2 % (w/w) of coffee beans while, after brewing, 650 kg of SCGs are left per 1 ton of coffee green bean (Ballesteros et al., 2014). Most of these residues have still no special use, being mostly discharged into the environment (Santos et al., 2016). The employment of coffee wastes in value-added applications could give therefore new life to these materials. To date, several applications have been tested for coffee residues, mainly as biofuels, composts, animal feed, biosorbents and enzymes (Martinez-Saez et al., 2017). However Oliveira and Franca (2015) reported that there is still a need for significant research to make the energy recovery of coffee residues a technically and economically viable option. Since these residues are obtained

at their processing facilities, the torrefaction pre-treatment can be carried out on-site, decreasing the transportation costs and improving the economic feasibility of the chain.
At the best of our knowledge, there are no papers using the desirability function approach to optimize the operating parameters of the torrefaction process. Thus, the aim of this study is to perform torrefaction for CC and SCG in a thermogravimetric analyzer, in order to find the optimization conditions based on minimizing the weight loss and maximizing the calorific gain. RSM was employed to examine the effects of torrefaction temperature, residence time, and heating rate on mass and energy yields of the solid products, investigating the chemical and physical properties of the torrefied biomass.

2. Materials and methods

2.1 Feedstock preparation

SCGs used in this study were supplied by a cafeteria in the province of Perugia (Italy) that uses a mixture of Arabica (Coffea arabica) and Robusta (Coffea canephora) coffee seeds. CC was provided by a coffee company located in Pavia, Italy. Each byproduct was dried in an oven at 105°C for 24 h until its water content was reduced to the mass fraction of about 5%. Both samples were ground using an ultra-centrifugal mill (mod. ZM200, Retsch) and sieved in order to obtain a particle size lower than 500 μm. The dried samples were then stored at room temperature in air-tight containers until use.

2.2 Torrefaction process

A thermogravimetric analyzer (TGA-701, LECO Co., USA) was employed to carry out the torrefaction tests. In each test, 0.3 g of raw material was placed in a ceramic crucible which was placed into the TGA. Nitrogen, at a flow rate of 3.5 L/min, was used as method process gas. The torrefaction test began at the temperature of 30°C and then, by a specified heating rate, the samples were heated to the required torrefaction temperature; the materials were held at a specific residence time, depending on the experimental conditions defined in the paragraph 2.5. The torrefied samples were extracted from the TGA when the temperature inside the furnace was lower than 100°C, in order to avoid any oxidation of the char.
The weight loss of the torrefied biomass was calculated using the following equation:

$$W_L = \left[\frac{M_0 - M_T}{M_0}\right] * 100 \qquad (1)$$

where W_L is the weight loss (%), M_0 is the initial mass of biomass before torrefaction and M_T is the residue mass after torrefaction.

2.3 Elemental analysis and energy value of biomass

Biomass properties were analyzed before and after torrefaction. In particular, raw materials were subjected to proximate, ultimate, and structural compositional analysis while torrefied samples were analyzed in terms of ultimate composition. The proximate analysis (moisture, ash, volatile matter, and fixed carbon content) was carried out in compliance with UNI EN 14774-2, UNI EN 14775, and UNI EN 15148 standard methods

by using a thermogravimetric analyzer (TGA-701, LECO Co., USA). Ultimate analysis was performed by using a LECO Truspec CHN analyser, in compliance with UNI EN 15104 standard method.
The fiber compositional analysis (cellulose, hemicellulose, lignin) was carried out according to NREL laboratory analytical procedures (Sluiter et al., 2008), following the method adopted in a previous study (Buratti et al., 2015).
HHV of the samples was calculated by applying the model developed by Friedl et al. (2005), from their C, H, and N contents. In particular HHV was attained using the following equation:

$$\mathrm{HHV}\ (\mathrm{kJ/kg}) = 3.55\mathrm{C}^2 - 232\mathrm{C} - 2230\mathrm{H} + 51.2\mathrm{C}*\mathrm{H} + 131\mathrm{N} + 20{,}600 \qquad (2)$$

where C, H, and N are the weight percentage obtained from the ultimate analysis.
All analytical procedures were performed in triplicate and a mean value was reported.

2.4 Thermogravimetric analysis

Thermal stability of the raw materials was evaluated by using a thermogravimetric analyzer (TGA-701, LECO Co., USA). Samples of about 0.2 g were heated from 30°C to 900°C under a nitrogen atmosphere, at a flow rate of 3.5 L/min and a constant heating rate of 10 °C/min.

2.5 Experimental design

A three-level, 3-factor Box–Behnken statistical screening design (BBD) was employed to determine the main effects, interaction effects, and quadratic effects of the torrefaction operating conditions (temperature, residence time, and heating rate) on the weight loss and HHV of biomass. BBD is an independent, quadratic design with no embedded factorial or fractional factorial points, where the variable combinations are at the midpoints of the edges of the variable space and at the center.
An experimental design with 15 experimental runs and three center points for the estimation of the pure error, replicated three times (three blocks) resulting in a total of 45 experiments, was used to optimize the chosen key variables.
Each independent factor used in this design was coded at three levels between +1, 0 and −1, corresponding to the minimum level, medium level, and maximum level. The low, medium, and high levels of each process factor were restricted to the region over which existing published Literature reported desirable values for other kind of biomass (Chen et al., 2015) and were also selected on the basis of the results, as obtained from preliminary experiments. The factors and their coded values are shown in Table 1.

[Table 1]

A non-linear regression method was used to fit the second order polynomial to the experimental data and to identify the relevant model terms. The general form of the predictive polynomial quadratic equation is given as:

$$Y = \beta_0 + \sum_{j=1}^{k} \beta_j x_j + \sum_{j=1}^{k} \beta_{jj} {x^2}_j + \sum_{i<j} \beta_{ij}\, x_i x_j \qquad (3)$$

where Y is the response (weight loss and HHV of torrefied biomass); β_0 is the intercept coefficient; βj, βjj and βij are interaction coefficients of linear, quadratic, and the second-order terms; k is the number of independent parameters (k = 3 in this study); x_j are the independent variables (temperature, residence time, heating rate).

2.6 Statistical analysis

Analysis of variance (ANOVA) and regression analysis were performed with Minitab 17.1.0 software, in order to evaluate the statistical significance of the full quadratic polynomial model, with a confidence level of 95% (P = 0.05). Experimental data was analyzed with several descriptive statistical analysis, such as p value, F value, degrees of freedom (DF), determination coefficient (R^2), adjusted determination of coefficient ($\mathrm{R}^2_{\mathrm{adj}}$), and predicted determination of coefficient ($\mathrm{R}^2_{\mathrm{pred}}$), in order to evaluate the statistical significance of the developed model. Then the model was employed for the construction of three dimensional response surface plots and for analyzing the interactive effect of each variable.

2.7 Multi-response optimization

Both responses (weight loss and HHV of the torrefied biomass) were concurrently optimized by multi-response analysis (Derringer and Suich, 1980) by using Derringer's desired function methodology. The approach of desirability function is first transform each response into a dimensionless individual desirability function (d_i), ranging from 0 to 1 (lowest to highest desirability). Then, the overall desirability function (D) is calculated by taking the geometric average of all individual desirability values (Eq. 4), as:

$$D = [d_1^{v1} * d_2^{v2} * \dots .* d_n^{vn}]^{1/n},\ 0 \leq vi \leq 1\ (i = 1,2,\dots,n),\ \sum_{i=1}^{n} vi = 1 \qquad (4)$$

where d_i is the individual desirability of the response Y_i (i = 1, 2, 3, ... , n), n is the number of responses and v_i represents the importance of each response.

In particular, if the D value is equal to 1, all responses achieve the target, while D equals 0 when any one response cannot reach the requirement.

The desired response of weight loss was the minimum of the target goal, whereas the desired HHV was the maximum. The same importance was assumed for each response during the optimization analysis. The software Minitab 17.1.0 was employed for the analysis of the results.

2.8. Validation of the model

Experiments at optimum conditions were carried out with three replications, in order to validate the optimized models, by comparing the experimental data with the predicted values.

3. Results and discussion

3.1 Characterization of raw and torrefied biomass

The basic properties of CC and SCGs are shown in Table 2. SCGs are characterized by the lowest ash, hemicellulose, and lignin contents, whereas they have the highest hemicellulose content

(33.4%). The higher volatile matter content of SCGs could be attributed to its higher content of holocellulose (sum of hemicellulose and cellulose). The lignocellulosic composition of both biomasses is in agreement with the Literature (Zarrinbakhsh et al., 2016; Ballesteros et al., 2014).

[Table 2]

The TGA curves of CC and SCGs show as their thermal degradation follows the typical trend for lignocellulosic biomass when exposed to heating until 900°C. The initial decrease in the TG curve is due to the moisture release, after which thermal degradation occurs in two steps. The main mass loss is observed during the second stage, at about 300ºC for both samples. At this stage, the depolymerization of cellulose and hemicellulose and the decomposition of some oils present in the sample occurs (Chiou et al., 2015). Then both the curves are characterized by a continuous slight devolatilization zone, where lignin decomposition and char formation occur. Comparing the TGA curves of CC and SCGs, it can be noticed that the devolatilization step of CC occurs earlier. This behaviour could probably be due to the higher content of lignin of CC, which decomposition happens in a wide range of temperatures, between 160°C and 900°C (Yang et al., 2006).

[Figure 1]

The average values of elemental composition of raw material and of the torrefied solid products are shown in Table 3, where it can be noticed that the weight percentage of C increases with increasing the torrefaction temperature and residence time, while heating rate has less influence, especially at the highest temperatures. At the same time the oxygen and hydrogen contents decrease considerably; this behaviour can be explained with the removal of volatile components, containing these atoms, during the torrefaction process. The elemental composition profiles are in agreement with expected changes in the biomass composition after torrefaction (Bach et al., 2016).

[Table 3]

The changes in the elemental composition of raw and torrefied biomass are also given in the Van Krevelen diagram (Fig. 2), which is a plot of atomic H/C ratio versus atomic O/C ratio. Each biomass shows a linear relationship in which it is clear from the slope of the regression that the torrefaction has more influence on hydrogen than on oxygen. Furthermore, the increase in carbon content improves the combustion properties because the low values of H/C and O/C ratios decrease thermodynamic losses and increase the calorific value (Chen et al., 2014).

[Figure 2]

3.2 Box–Behnken design and analysis

A total number of 45 runs, including nine centre points (used to determine the experimental error) was carried out, in order to evaluate the optimum conditions and to study the influence of the process variables on the torrefaction process. Tables 4 and 5 show the experimental conditions with their respective experimental responses, together with the predicted values from the BBD model. The trials were performed in random order, for minimizing the effects of unexpected variability on the observed responses.

[Table 4]

[Table 5]

By applying multiple regression analysis on the experimental data, the relationship between the response variables and the input variables was expressed by second order polynomial equations with interaction terms. The final models generated in coded factors are shown below:

$$W_L\,(CC) = 28.808 + 14.753X_1 + 4.265X_2 + 0.866X_3 - 1.141X^2{}_1 - 0.623X^2{}_2 + 0.908X^2{}_3 - 0.302X_1X_2 - 0.755X_1X_3 + 0.246X_2X_3 \quad (5)$$

$$W_L\,(SCGs) = 24.694 + 15.725X_1 + 4.110X_2 + 1.118X_3 - 2.164X^2{}_1 + 0.357X^2{}_2 + 0.213X^2{}_3 + 0.419X_1X_2 - 0.123X_1X_3 - 0.852X_2X_3 \quad (6)$$

$$HHV\,(CC) = 22215.6 + 1923.9X_1 + 305.7X_2 - 41.7X_3 + 408.4X^2{}_1 + 403.6X^2{}_2 + 285.7X^2{}_3 - 271.6X_1X_2 - 370.4X_1X_3 + 354.5\,X_2X_3 \quad (7)$$

$$HHV\,(SCGs) = 27409.4 + 3859.5X_1 + 403.3X_2 + 412.6X_3 - 246.8X^2{}_1 + 551.2X^2{}_3 + 279.5X^2{}_3 - 477.4X_1X_2 - 227.3X_1X_3 - 346.5X_2X_3 \quad (8)$$

Analysis of variance (ANOVA) was performed for adequacy and fitness of predicted models. In particular, the influence of each factor on the model was evaluated by the Fisher's statistical test (F-test). The results of ANOVA, reported in Table 6, show that the Fisher's F-values for the HHV and WL models of CC and SCGs are 143.12, 846.97, 419.85, and 1080.20 respectively, demonstrating that the regression models are highly significant. Furthermore, the corresponding p values suggest if F values are large enough to show statistical significance. At this regard, all p values are markedly lower than 0.05 (<0.0001), confirming that the models are statistically significant.

[Table 6]

The adequacy of the model was further analyzed by the evaluation of the determination coefficient (R^2) and the lack of fit (LOF) test. In particular, a model can be considered acceptable if the R^2 value is higher than 0.95, meaning that up to 95% of the data variability could be explained by the model (Bajar et al., 2016). The values of R^2 of the HHV and WL models of CC and SCGs are 0.9795, 0.9965, 0.9929, and 0.9945 respectively, validating the precision of the deduced models. However, since R^2 is sensitive to the degree of freedom, increasing with adding more model terms, the adjusted coefficient of determination (R^2_{adj}) value is more useful to check the model adequacy, correcting the R^2 value for the number of terms in the model (Glyk et al., 2015). All values were higher than 0.95, confirming again the accuracy of the proposed models with the responses in the specified field conditions. Furthermore the predicted R^2 (R^2_{pred}) and adjusted R^2 values were in reasonable agreement, being within 0.2 of each other for all the models (Lou et al., 2013). It indicated that the proposed regression model adequately represents the actual relationship among the chosen variables.

The acceptability of the model can be verified by the LOF test, which compares the residual error (the error associated with the fitted model) to the pure error from the replicated design points (Luo et al., 2010). A *p*-value higher than 0.05 means that the LOF is insignificant relative to the pure error. There is a chance of 15.8%, 23.5%, 47.8%, and 6% for the HHV and WL models of CC and SCGs that the LOF F-values could occur due to noise, highlighting a non-significant shortage of the models in the prediction of experimental data.

The adequacy of the developed mathematical models was also verified by constructing diagnostic plots, such as predicted versus actual values. Fig. 3 shows that data points on this plot lie very close to the straight line, indicating a fair agreement between the experimental data and the model and a good response to the model.

[Figure 3]

Residuals were also investigated, in order to verify if they fit a normal distribution. The normality assumption was evaluated by the normal probability plot of the residuals, as shown in Fig. 4. Since the regression data on the plot are very close to a straight line (Swamy et al., 2014), it is possible to confirm that data was normally distributed and the variation of the predicted from the actual values was random.

[Figure 4]

3.3 Effect of independent variables on the torrefaction process

The influence of the independent variables on the responses and their interactions were evaluated by plotting three dimensional (3D) response surface graphs, as shown in Fig. 5 and 6.

The response surface plots showed the influence of any two variables on the process, while the third variable was kept as constant. The nonlinear nature of 3D response surfaces plots indicate the interactions between each of the independent variables (temperature, residence time, and heating rate) in determining the weight loss and the calorific gain.

[Figure 5]

[Figure 6]

3.3.1 Effect on weight loss

Fig. 5 and 6 show the effects of torrefaction temperature (X_1), residence time (X_2), and heating rate (X_3) on the weight loss of CC and SCGs. Both samples had weight loss that depended more on temperature than residence time and heating rate. In particular, by comparing the p-values of the regression coefficients (tab. 6), the effects on weight loss for both samples could be sequenced as torrefaction temperature > residence time > heating rate. This result is in agreement with previous studies that showed the greater influence of temperature than residence time and heating rate on the weight loss (Chiou et al., 2015; Mundike et al., 2016; Nam and Capareda, 2015). The independent variables significantly ($p < 0.0001$) influence the weight loss of CC in a linear and quadratic manner while, for SCGs, only torrefaction temperature has a significant impact between the quadratic terms. Among the interaction variable coefficients, only residence time-heating rate and temperature-heating rate were found to be significant in determining the response of SCGs and CC, respectively.

All independent variables have positive effect in linear terms for both samples, while temperature showed a negative effect on its quadratic terms in both cases. The interactive effects between temperature-residence time and residence time-heating rate showed positive effects for SCGs and CC, respectively. At this regard, Literature studies show that the weight loss model could depend only on torrefaction temperature and residence time (Na et al., 2013) or on higher order interaction terms (Medic et al., 2012) as a function of the kind of the tested biomass.

Fig. 5 and 6 show that the weight loss of CC and SCGs is intensified with increasing of temperature, residence time, and heating rate. In particular, over the temperature range of 220–300 °C, the weight loss increases from 8.6-16.3% to 38.4–44.9% and from 4.5%-10.3% to 34.6%-42.1% for CC and SCGs, respectively. Therefore, at the same torrefaction temperature, the average weight loss of CC is much higher than that of SCGs. This difference is mainly due to the different chemical composition. In the temperature range of torrefaction, thermal degradation of hemicellulose is more severe than the decomposition of cellulose and lignin (Mundike et al., 2016). Therefore biomass with higher content of hemicellulose, such as SCGs, should be characterized by higher values of weight loss. However, the higher ash content of CC could contribute to increase its thermal decomposition (Uemura et al., 2011), causing the highest weight loss. Furthermore, the hemicellulose fraction in SCGs has a different chemical composition with respect the one of CC, because the concentration of the most reactive hemicellulose (xylan) is less with a high proportion of glucomannan (Ballesteros et al., 2014), less reactive than xylan (Prins et al., 2006).

The residence time has a positive influence on the weight loss during the torrefaction process because a longer hold period allows more time for the formation of oxygenated volatiles (Mundike et al., 2016), with higher weight loss. The influence of heating rate on both biomass (CC and SCGs) shows a positive effect on the weight loss, for identical temperature and residence time. This trend could be due to an increased rate of depolymerization and dehydration of lignocellulosic polymers into volatiles (Supramono et al., 2015).

3.3.2 Effect on HHV

The response surface plots estimating the specific surface area of HHV versus independent variables are also shown in Fig. 5 and 6. For both biomass, HHV is significantly affected ($p < 0.0001$) by the torrefaction temperature in a linear manner. From the regression analysis of the model equation (Tab. 6), it is clear that the linear, square as well as the interaction effects of the independent process variables are highly significant ($p < 0.0001$) on the HHV of SCGs. Instead, the HHV of torrefied CC is not significantly affected ($p=0.419$) by the linear term of heating rate. According to the F-values, the linear term of heating rate has the most significant influence on the HHV of SCGs and CC. Among the interaction terms, temperature-residence time and temperature-heating rate has a larger significant effect on the HHV of SCGs and CC, respectively. Furthermore, among the quadratic terms, residence time and temperature show the most influence on the calorific value of SCGs and CC, respectively.

Both samples show an increase in char HHV in response to an increase in temperature and residence time, as suggested by the positive linear coefficients in the equations 7 and 8, in agreement with those of other studies (Rousset et al., 2011; Chen et al., 2012). Among the linear terms, only heating rate for CC has a negative effect, despite it does not statistically influence HHV. Full quadratic analysis also shows that temperature interacts negatively with residence time and heating rate for both biomass. These significant interaction means that the effects of residence time and heating rate on HHV depend on the level of torrefaction temperature. Among the squared terms, only temperature for SCGs shows a negative effect on the HHV, indicating that the response is described by a convex surface and that high values tend to decrease char HHV.

Analyzing the influence of torrefaction temperature for the same conditions (e.g. residence time of 40 min and heating rate of 5°C/min) on the calorific gain of CC and SCGs, from tables 4 and 5 it can be seen that CC has the largest HHV increase (+10.8%) compared to the one of SCGs (+6.9%) at 220°C, while the trend is the opposite at 300°C (SCGs: +43.3%, CC: +35.5%). These results are in agreement with the ones reported by Chen et al. (2015) for other kind of biomass, for which the calorific gain can reach up to about 60%. Moreover, this difference between the samples is probably due to the differences in the polymeric structure, causing a different reduction of low-energy chemical bonds, such as H–C and O–C, and increase in a high-energy chemical bond (C–C) (Yang et al., 2015).

3.4 Determination and validation of optimum conditions

Previous studies on the optimization of the torrefaction process were mainly based on the evaluation of the energy yield of the product (Chin et al., 2013; Asadullah et al., 2014; Kim et al., 2013). Energy yield is defined as the product of the char yield and the ratio of the HHV of torrefied biomass to the HHV of the raw biomass. It indicates the amount of energy of the raw biomass that remains in the torrefied product.

However, as reported by Lee and Lee (2014), the evaluation of the energy yield is not sufficient to properly optimize the operating conditions of torrefaction. In fact, with the increasing of the severity of the process, the energy yield generally decreases, implying that the net usable energy of raw material is reduced. Therefore, the optimized torrefaction condition is the one which allows to minimize the weight loss and maximize the calorific value of the product. Since currently an accepted method to optimize the torrefaction process does not exist (Chin et al., 2013), it was decided to apply the Derringer's desirability function method.

Composite desirability evaluates how the settings optimize a set of responses overall (Mahanty et al., 2014). In this case, the importance parameter of 1 and equal weightages were given for both responses (W_L and HHV).

As shown in Fig. 7, employing the Derringer's desirability function methodology, the optimum level of the independent variables was obtained; in particular, the maximum desirability is predicted to be 52.1% and 56.2% at 271.7°C and 256.0°C torrefaction temperature, 20 min residence time, 5°C/min and 25°C/min heating rate for CC and SCGs, respectively.

[Figure 7]

In order to verify the results of the model, a torrefaction treatment for both biomass was carried out under the optimized conditions. Experiments were performed in triplicate and the average values are reported in Tab.

7. Results confirm the suitability of the developed quadratic models because the experimental findings are in close agreement with the predicted values.

[Table 7]

4. Conclusion

Torrefaction tests carried out in this study allowed to observe the behaviour of CC and SCGs under a broad range of torrefaction conditions, with only limited amount of samples and effort required to obtain a large matrix of results. TGA tests provided the degree of torrefaction as a result of the operating conditions. These tests not only provided an idea how material would behave during torrefaction, but also the operating conditions for torrefaction tests at large scale.

In particular, the Box-Behnken response surface design proves to be very useful in determining the optimal conditions for the torrefaction process of CC and SCGs. Response surface models of weight loss and Higher Heating Value depend on the specific biomass, with most models containing a temperature–time interaction, square of temperature, or square of time terms.

Analysis of variance showed high R^2 values, indicating a good fit of the regression models to the experimental data. CC has the highest weight loss, while SCGs shows generally highest values of calorific gain. The optimum conditions for the torrefaction process resulted in a weight loss of 28.7% and 21.6% and a calorific gain of 26.7% and 29.9% for CC and SCGs respectively. Under the optimized conditions obtained from the Derringer's desired function methodology, the experimental values are in close agreement with the predicted ones.

References

- Asadullah, M., Adi, A.M., Suhada, N., Malek, N.H., Saringat, M.I., Azdarpour, A., 2014. Optimization of palm kernel shell torrefaction to produce energy densified biocoal. Energy Convers. Manage. 88, 1086–1093.
- Aziz, M.A., Sabil, K.M., Uemura, Y., Ismail, L., 2012. A study on torrefaction of oil palm biomass. J. Appl. Sci. 12, 1130–1135.
- Bach, Q.V., Chen, W.H., Chu, Y.S., Skreiberg, O., 2016. Predictions of biochar yield and elemental composition during torrefaction of forest residues. Bioresour. Technol. 215, 239–246.
- Bajar, S., Singh, A., Kaushik, C.P., Kaushik, A., 2016. Evaluation and statistical optimization of methane oxidation using rice husk amended dumpsite soil as biocover. Waste Manage. 53, 136–143.
- Ballesteros, L.F., Teixeira, J.A., Mussatto, S.I., 2014. Chemical, functional, and structural properties of spent coffee grounds and coffee silverskin. Food Bioprocess Technol. 7, 3493–3503.
- Buratti, C., Barbanera, M., Lascaro, E., 2015. Ethanol production from vineyard pruning residues with steam explosion pretreatment. Environ. Prog. Sustain. Energy 34, 802–809.
- Chen, W.H., Kuo, P.C., 2011. Torrefaction and co-torrefaction characterization of hemicellulose, cellulose and lignin as well as torrefaction of some basic constituents in biomass. Energy 36, 803–811.
- Chen, W.H., Lu, K.M., Tsai, C.M., 2012. An experimental analysis on property and structure variations of agricultural wastes undergoing torrefaction. Appl. Energy 100, 318–325.

- Chen, W.-H., Peng, J., Bi, X.T., 2015. A state-of-the-art review of biomass torrefaction, densification and applications. Renew. Sustain. Energy Rev. 44, 847–866.
- Chen, Y., Yang, H., Yang, Q., Hao, H., Zhu, B., Chen, H., 2014. Torrefaction of agriculture straws and its application on biomass pyrolysis poly-generation. Bioresour. Technol. 156, 70–77.
- Chin, K.L., H'ng, P.S., Go, W.Z., Wong, W.Z., Lim, T.W., Maminski, M., Paridah, M.T., Luqman, A.C., 2013. Optimization of torrefaction conditions for high energy density solid biofuel from oil palm biomass and fast growing species available in Malaysia. Ind. Crop. Prod. 49, 768–774.
- Chiou, B.S., Valenzuela-Medina, D., Bilbao-Sainz, C., Klamczynski, A.K., AvenaBustillos, R.J., Milczarek, R.R., Du, W.X., Glenn, G.M., Orts, W.J., 2015. Torrefaction of pomaces and nut shells. Bioresour. Technol. 177, 58–65.
- Costa, N.R., Lourenco, J., Pereira, Z.L., 2011. Desirability function approach: a review and performance evaluation in adverse conditions. Chemom. Intell. Lab. Syst. 107, 234–244.
- Cotana, F., Buratti, C., Barbanera, M., Lascaro, E., 2015. Optimization of the steam explosion and enzymatic hydrolysis for sugars production from oak woods. Bioresour. Technol. 198, 470–477.
- Cruz, R., Mendes, E., Torrinha, A., Morais, S., Pereira, J.A., Baptista, P., Casal, S., 2014. Revalorization of spent coffee residues by direct agronomic approach. Food Res. Int. 73, 190–196.
- Derringer, G., Suich, R., 1980. Simultaneous optimization of several response variables. J. Qual. Technol. 12, 214-219.
- Fan, L., Soccol, A.T., Pandey, A., Soccol, C.R., 2003. Cultivation of Pleurotus mushrooms on Brazilian coffee husk and effects of caffeine and tannic acid. Micología Aplicada Int. 15, 15–21.
- Friedl, A., Padouvas, E., Rotter, H., Varmuza, K., 2005. Prediction of heating values of biomass fuel from elemental composition. Anal. Chim. Acta. 544, 191–198.
- Glyk, A., Solle, D., Scheper, T., Beutel, S., 2015. Review Optimization of PEG–salt aqueous two-phase systems by design of experiments. Chemom. Intell. Lab. Syst. 149, 12–21.Goldfarb, J.L., Liu, C., 2013. Impact of blend ratio on the co-firing of a commercial torrefied biomass and coal via analysis of oxidation kinetics. Bioresour. Technol. 149, 208–215.
- International Coffee Organization, 2016. Trade Statistics Tables: World coffee consumption. Avalable at: www.ico.org/prices/new-consumption-table.pdf (accessed 9 March 2017).
- Kim, Y.H., Na, B.I., Lee, S.M., Lee, H.W., Lee, J.W., 2013. Optimal condition for torrefaction of eucalyptus by response surface methodology. J. Korean Wood Sci. Technol. 41, 497–506.
- Lee, J.W., Kim, Y.H., Lee, S.M., Lee, H.W., 2012. Optimizing the torrefaction of mixed softwood by response surface methodology for biomass upgrading to high energy density. Bioresour. Technol. 116, 471–476.
- Lee, S.M., Lee, J., 2014. Optimization of biomass torrefaction conditions by the Gain and Loss method and regression model analysis, Bioresour. Technol. 172, 438-443.
- Lou, H.,Li, W., Li, C., Wang, X., 2013. Systematic investigation on parameters of solution blown micro/nanofibers using response surface methodology based on Box-Behnken design, J. Appl. Polym. Sci. 130, 1383-1391.
- Luo, S.Y., Xiao, B., Hu, Z.Q., Liu, S.M., 2010. Effect of particle size on pyrolysis of single-component municipal solid waste in fixed bed reactor. Int. J. Hydrogen Energy 35 (1), 93–97.

- Mahanty, B., Zafar, M., Han, M.J., Park, H.S., 2014. Optimization of co-digestion of various industrial sludges for biogas production and sludge treatment: Methane production potential experiments and modeling. Waste Manage. 34, 1018–1024.
- Maran, J. P., Manikandan, S., 2012. Response surface modeling and optimization of process parameters for aqueous extraction of pigments from prickly pear (Opuntia ficus-indica) fruit. Dyes and Pigments, 95, 465–472.
- Martinez-Saez, N., Garcia, A.T., Perez, I.D., Rebollo-Hernanz, M., Mesias, M., Morales, F.J., Martin-Cabrejas, M.A., Del Castillo, M.D., 2017. Use of spent coffee grounds as food ingredient in bakery products. Food Chem. 216, 114-122.
- McKendry, P., 2002. Energy production from biomass (part 2): conversion technologies. Bioresour. Technol. 83 (47–54), 8.
- Medic, D., Darr, M., Shah, A., Potter, B., Zimmerman, J., 2012. Effects of torrefaction process parameters on biomass feedstock upgrading. Fuel 91, 147–154.
- Mundike, J., Collard, F.X., Gorgens, J.F., 2016. Torrefaction of invanse alien plants: Influence of heating rate and other conversion parameters on mass yield and higher heating value. Bioresour. Technol. 209, 90–99.
- Murthy, P.S., Madhava Naidu, M., 2012. Sustainable management of coffee industry by-products and value addition: a review. Resour. Conserv. Recyl. 66, 45–58.
- Myers, R.H., Montgomery, D.C., Anderson-Cook, C.M., 2009. Response Surface Methodology: Process and Product Optimization Using Designed Experiments, second ed. John Wiley & Sons, New York.
- Na, B.I., Kim, Y.H., Lim, W.S., Lee, S.M., Lee, H.W., Lee, J.W., 2013. Torrefaction of oil palm mesocarp fiber and their effect on pelletizing. Biomass Bioenergy 52, 159–165.
- Nam, H., Capareda, S., 2015. Experimental investigation of torrefaction of two agricultural wastes of different composition using RSM (response surface methodology). Energy 91, 507–516.
- Oliveira, L.S., Franca, A.S., 2015. An overview of the potential uses for coffee husks, in: Preedy, V.R. (Ed), Coffee in health and disease prevention, vol 31, Academic Press, San Diego, pp 283–291.
- Phanphanich, M., Mani, S., 2011. Impact of torrefaction on the grindability and fuel characteristics of forest biomass. Bioresour. Technol. 102, 1246–1253.
- Poudel, J., Ohm, T., Lee, S., Oh, S.C., 2015. A study on torrefaction of sewage sludge to enhance solid fuel qualities. Waste Manage. 40, 112-118Prins, M.J., Ptasinski, K.J., Janssen, F.J.J.G., 2006. Torrefaction of wood – Part 2. Analysis of products. J. Anal. Appl. Pyrol. 77 (1), 35–40.
- Rousset, P., Aguiar, C., Labbe, N., Commandre, J.M., 2011. Enhancing the combustible properties of bamboo by torrefaction. Bioresour. Technol. 102, 8225–8231.
- Santos, C., Fonseca, J., Aires, A., Coutinho, J., Trindade, H., 2016. Effect of different rates of spent coffee grounds (SCG) on composting process, gaseous emissions and quality of end-product. Waste Manage 59, 37-47.
- Shang, L., Ahrenfeldt, J., Holm, J.K., Sanadi, A.R., Barsberg, S., Thomsen, T., Stelte, W., Henriksen, U.B., 2012. Changes of chemical and mechanical behavior of torrefied wheat straw. Biomass Bioenergy 40, 63–70.
- Sluiter, A., Hames, B., Ruiz, R., Scarlata, C., Sluiter, J., Templeton, D., Crocker, D., 2008. Determination of Structural Carbohydrates and Lignin in Biomass. National Renewable Energy Laboratory (NREL)

Laboratory Analytical Procedures (LAP) for Standard Biomass Analysis. <http://www.nrel.gov/docs/gen/fy13/42618.pdf>.
- Supramono, D., Merry Devina, Y., Tristantini, D., 2015. Effect of heating rate of torrefaction of sugarcane bagasse on its physical characteristics. Int. J. Technol. 7, 1084-1093.
- Swamy, G.J., Sangamithra, A., Chandrasekar, V., 2014. Response surface modeling and process optimization of aqueous extraction of natural pigments from Beta vulgaris using Box-Behnken design of experiments, Dyes Pigments 111, 64–74.
- Uemura, Y., Omar, W., Othman, N.A., Yusup, S., Tsutsui, T., 2011. Torrefaction of oil palm wastes. Fuel 90, 2585–2591.
- Viacava, G.E., Roura, S.I., Agüero, M.V., 2015. Optimization of critical parameters during antioxidants extraction from butterhead lettuce to simultaneously enhance polyphenols and antioxidant activity. Chemom. Intell. Lab. Syst. 146, 47–54.
- Yan, W., Acharjee, T.C., Coronella, C.J., Vasquez, V.R., 2009. Thermal pretreatment of lignocellulosic biomass. Environ. Prog. Sustain. Energy 28, 435.
- Yang, H., Yan, R., Chen, H., Zheng, C., Lee, D.H., Liang, D.T., 2006. In-depth investigation of biomass pyrolysis based on three major components: hemicellulose, cellulose and lignin. Energy Fuels 20, 388–393.
- Yang, W., Shimanouchi, T., Iwamura, M., Takahashi, Y., Mano, R., Takashima, K., Tanifuji, T., Kimura, Y., 2015. Elevating the fuel properties of Humulus lupulus, Plumeria alba and Calophyllum inophyllum L. through wet torrefaction. Fuel 146, 88–94.
- Zarrinbakhsh, N., Arturo Rodriguez-Uribe, T.W., Misra, M., Mohanty, A.K., 2016. Characterization of Wastes and Coproducts from the Coffee Industry for Composite Material Production. BioResources 11 (3), 7637-7653.

Figure Captions

- Fig. 1. TG curves for CC and SCGs samples at a heating rate of 10 °C/min
- Fig. 2. Van Krevelen plot of atomic H/C ratio versus atomic O/C ratio of raw and torrefied CC (a) and SCGs (b).
- Fig. 3. Relationship between predicted and actual values of a) W_L of CC, b) HHV of CC, c) W_L of SCGs, d) HHV of SCGs,
- Fig. 4. Normal probability plots of residuals of a) W_L of CC, b) HHV of CC, c) W_L of SCGs, d) HHV of SCGs
- Fig. 5. 3D response surface plots of WL and HHV showing the effect of process variables for CC.
- Fig. 6. 3D response surface plots of WL and HHV showing the effect of process variables for SCGs
- Fig. 7. Optimization plots of operating variables for a) CC and b) SCGs.

Highlights

- Response surface methodology was applied for optimization the torrefaction process
- Reaction temperature, residence time and heating rate were the independent variables
- Calorific gain was 26.7% and 29.9% for CC and SCGs under the optimum conditions
- Weight loss was 28.7% and 21.6% for CC and SCGs under the optimum conditions

Table 1

Table 1. Independent process variables, range and levels in experimental design

Independent variables	**Symbols**	**Coded levels**		
		-1	*0*	*+1*
Temperature (°C)	X_1	220	260	300
Residence time (min)	X_2	20	40	60
Heating rate (°C/min)	X_3	5	15	25

Table 2

Table 2. Proximate, fiber and calorific analyses of CC and SCGs

Raw material	CC	SCGs
Volatile matter (%, db)	79.30	80.58
Fixed carbon (%, db)	14.76	16.90
Ash (%, db)	5.94	2.52
Cellulose (%, db)	22.83	12.31
Hemicellulose (%, db)	19.30	33.44
Lignin (%, db)	28.59	24.52
HHV (MJ/kg, db)	18.62	21.69

Table 3

Table 3. Elemental composition of raw and torrefied materials.

Material	Temperature (°C)	Residence time (min)	Heating rate (°C/min)	Elemental analysis (%)			
				N	C	H	O[a]
CC							
	Raw material			*2.4*	*45.8*	*8.1*	*43.7*
	220	20	15	2.5	49.7	7.7	40.0
	220	40	5	2.9	50.2	7.6	39.3
	220	40	25	3.1	51.2	7.4	38.3
	220	60	15	3.0	51.2	7.5	38.2
	260	20	5	3.1	53.9	7.0	36.0
	260	20	25	3.2	53.7	6.7	36.4
	260	40	15	3.2	53.2	7.1	36.5
	260	60	5	3.3	55.9	6.3	34.4
	260	60	25	3.3	56.6	6.5	33.5
	300	20	15	3.6	60.0	6.3	30.2
	300	40	5	3.9	61.0	5.7	29.4
	300	40	25	3.8	57.7	6.5	32.0
	300	60	15	4.0	60.2	5.7	30.0
SCGs							
	Raw material			*1.9*	*50.7*	*9.4*	*37.9*
	220	20	15	2.4	52.9	9.0	35.8
	220	40	5	2.4	53.6	9.0	35.1
	220	40	25	2.5	55.3	8.9	33.4
	220	60	15	2.6	55.5	9.0	33.0
	260	20	5	3.0	59.5	8.7	28.8
	260	20	25	2.7	62.7	8.5	26.1
	260	40	15	3.0	60.9	8.3	27.8
	260	60	5	2.9	63.2	7.9	26.0
	260	60	25	3.1	63.8	8.0	25.1
	300	20	15	3.0	68.6	7.9	20.5
	300	40	5	3.8	68.1	7.4	20.7
	300	40	25	3.4	68.8	7.2	20.7
	300	60	15	3.6	69.6	7.1	19.6

[a] Oxygen was calculated by difference

Table 4

Table 4. Experimental responses of the torrefaction process of CC

Run Order	X1 (°C)	X2 (min)	X3 (°C/min)	Weight loss (%)			HHV (MJ/kg)		
				Actual	Predicted	Residual	Actual	Predicted	Residual
1	220	40	5	11.41	12.28	0.87	20.84	20.66	0.18
2	220	40	25	15.90	15.52	0.38	21.32	21.31	0.00
3	300	40	25	44.12	43.52	0.60	24.41	24.42	0.01
4	220	20	15	8.73	7.80	0.93	20.59	20.53	0.07
5	260	60	5	33.79	32.32	1.47	23.11	23.07	0.04
6	300	20	15	38.37	37.91	0.46	25.27	24.92	0.36
7	300	60	15	44.95	45.84	0.89	24.91	24.98	0.08
8	260	60	25	34.86	34.55	0.31	23.44	23.35	0.09
9	260	40	15	28.25	28.89	0.64	22.33	22.21	0.12
10	300	40	5	42.77	43.30	0.53	25.09	25.24	0.15
11	260	40	15	29.05	28.89	0.16	22.06	22.21	0.15
12	220	60	15	16.21	16.94	0.73	21.41	21.68	0.27
13	260	20	25	24.84	25.53	0.69	22.25	22.38	0.12
14	260	20	5	23.85	24.29	0.44	22.43	22.82	0.39
15	260	40	15	29.35	28.89	0.46	22.54	22.21	0.32
16	300	60	15	45.04	45.72	0.68	24.94	24.99	0.05
17	220	40	5	11.70	12.16	0.46	20.82	20.66	0.16
18	260	40	15	28.94	28.77	0.17	22.18	22.22	0.04
19	300	20	15	38.39	37.79	0.60	25.26	24.92	0.33
20	260	60	25	34.89	34.43	0.46	23.80	23.35	0.45
21	260	40	15	28.54	28.77	0.23	22.25	22.22	0.03
22	260	40	15	28.61	28.77	0.16	22.31	22.22	0.09
23	300	40	25	43.98	43.40	0.58	24.09	24.43	0.33
24	260	20	25	23.82	25.41	1.59	22.33	22.38	0.05
25	260	20	5	23.78	24.17	0.39	22.60	22.82	0.22
26	220	20	15	8.67	7.68	0.99	20.58	20.53	0.05
27	220	60	15	16.52	16.82	0.30	21.43	21.69	0.26
28	300	40	5	42.85	43.18	0.33	25.10	25.25	0.15
29	220	40	25	15.59	15.40	0.19	21.33	21.32	0.01
30	260	60	5	33.37	32.21	1.16	23.08	23.08	0.00
31	300	20	15	38.45	37.79	0.66	25.14	24.91	0.23
32	260	20	25	24.32	25.41	1.09	22.27	22.38	0.11
33	300	60	15	44.75	45.72	0.97	24.85	24.98	0.13
34	220	40	25	15.66	15.40	0.26	21.33	21.31	0.01
35	220	60	15	16.13	16.82	0.69	21.29	21.68	0.39
36	260	40	15	29.13	28.77	0.36	21.93	22.21	0.29
37	220	40	5	11.84	12.16	0.32	20.94	20.65	0.29
38	220	20	15	8.31	7.68	0.63	20.66	20.52	0.14
39	260	20	5	24.10	24.17	0.07	22.54	22.81	0.28
40	300	40	25	43.87	43.40	0.47	24.13	24.42	0.29
41	260	40	15	29.52	28.77	0.75	22.28	22.21	0.07
42	260	60	25	34.55	34.43	0.12	23.70	23.34	0.35
43	300	40	5	43.21	43.18	0.03	25.52	25.24	0.27
44	260	40	15	27.88	28.77	0.89	22.07	22.21	0.15
45	260	60	5	32.94	32.21	0.73	23.33	23.07	0.25

Table 5

Table 5. Experimental responses of the torrefaction process of SCGs

Run Order	X_1 (°C)	X_2 (min)	X_3 (°C/min)	Weight loss (%)			HHV (MJ/kg)		
				Actual	Predicted	Residual	Actual	Predicted	Residual
1	220	40	5	5.54	5.83	0.29	23.47	23.01	0.46
2	220	40	25	7.90	8.31	0.41	24.23	24.29	0.06
3	300	40	25	40.04	39.51	0.53	31.21	31.55	0.34
4	220	20	15	4.56	3.52	1.04	22.89	23.04	0.15
5	260	60	5	30.15	29.16	0.99	28.66	28.65	0.02
6	300	20	15	34.75	34.14	0.61	32.16	31.72	0.45
7	300	60	15	41.95	43.19	1.24	31.63	31.57	0.06
8	260	60	25	30.27	29.69	0.58	28.81	28.78	0.03
9	260	40	15	24.85	24.75	0.10	27.50	27.48	0.03
10	300	40	5	37.70	37.52	0.18	30.90	31.18	0.28
11	260	40	15	24.89	24.75	0.14	27.53	27.48	0.05
12	220	60	15	10.52	10.90	0.38	24.28	24.80	0.52
13	260	20	25	22.40	23.18	0.78	28.84	28.66	0.17
14	260	20	5	18.42	19.24	0.82	27.01	27.15	0.14
15	260	40	15	24.49	24.75	0.26	27.71	27.48	0.23
16	300	60	15	42.27	43.07	0.80	31.59	31.44	0.15
17	220	40	5	5.43	5.70	0.27	23.20	22.88	0.32
18	260	40	15	24.39	24.62	0.23	27.54	27.35	0.19
19	300	20	15	34.49	34.01	0.48	31.78	31.59	0.20
20	260	60	25	30.20	29.57	0.63	28.87	28.65	0.22
21	260	40	15	24.14	24.62	0.48	27.00	27.35	0.35
22	260	40	15	25.37	24.62	0.75	27.33	27.35	0.02
23	300	40	25	39.37	39.39	0.02	31.08	31.43	0.35
24	260	20	25	22.32	23.05	0.73	28.53	28.54	0.00
25	260	20	5	18.43	19.11	0.68	26.64	27.02	0.38
26	220	20	15	4.61	3.40	1.21	22.96	22.91	0.05
27	220	60	15	10.04	10.78	0.74	24.50	24.68	0.17
28	300	40	5	37.60	37.40	0.20	31.13	31.06	0.07
29	220	40	25	8.08	8.18	0.10	24.19	24.16	0.03
30	260	60	5	29.80	29.03	0.77	28.58	28.52	0.06
31	300	20	15	34.66	34.11	0.55	31.79	31.64	0.15
32	260	20	25	22.04	23.15	1.11	28.68	28.59	0.10
33	300	60	15	42.18	43.17	0.99	31.68	31.49	0.19
34	220	40	25	8.39	8.28	0.11	24.37	24.21	0.16
35	220	60	15	10.35	10.88	0.53	24.63	24.73	0.10
36	260	40	15	24.51	24.72	0.21	27.72	27.40	0.32
37	220	40	5	5.39	5.80	0.41	23.21	22.93	0.28
38	220	20	15	4.27	3.50	0.77	22.67	22.96	0.29
39	260	20	5	18.65	19.21	0.56	26.93	27.07	0.14
40	300	40	25	39.95	39.49	0.46	31.11	31.48	0.36
41	260	40	15	24.97	24.72	0.25	26.99	27.40	0.41
42	260	60	25	30.51	29.67	0.84	29.11	28.70	0.41
43	300	40	5	37.53	37.50	0.03	31.19	31.11	0.08
44	260	40	15	24.64	24.72	0.08	27.37	27.40	0.03
45	260	60	5	29.99	29.13	0.86	28.22	28.57	0.35

Table 6

Table 6. ANOVA of response surface quadratic models

Source	DF	F-value	Prob > F
W_L, CC			
Model	9	846.97	<0.0001
X_1	1	8513.19	<0.0001
X_2	1	711.60	<0.0001
X_3	1	29.35	<0.0001
X^2_1	1	23.50	<0.0001
X^2_2	1	7.02	0.012
X^2_3	1	14.89	0.001
X_1X_2	1	1.78	0.191
X_1X_3	1	11.15	0.002
X_2X_3	1	1.18	0.285
Lack of fit (LOF)	27	1.82	0.235
R^2 = 0.9965, R^2_{adj}= 0.9953, R^2_{pred}= 0.9931			
HHV, CC			
Model	9	143.12	<0.0001
X_1	1	1427.12	<0.0001
X_2	1	36.03	<0.0001
X_3	1	0.67	0.419
X^2_1	1	29.68	<0.0001
X^2_2	1	28.98	<0.0001
X^2_3	1	14.52	0.001
X_1X_2	1	14.22	0.001
X_1X_3	1	26.45	<0.0001
X_2X_3	1	6.06	0.019
Lack of fit (LOF)	27	2.25	0.158
R^2 = 0.9795, R^2_{adj}= 0.9726, R^2_{pred}= 0.9603			
W_L, SCGs			
Model	9	1080.20	<0.0001
X_1	1	10954.35	<0.0001
X_2	1	748.13	<0.0001
X_3	1	55.40	<0.0001
X^2_1	1	95.77	<0.0001
X^2_2	1	2.61	0.116
X^2_3	1	0.93	0.342
X_1X_2	1	3.89	0.057
X_1X_3	1	0.34	0.566
X_2X_3	1	16.07	<0.0001
Lack of fit (LOF)	27	3.54	0.060
R^2 = 0.9972, R^2_{adj}= 0.9963, R^2_{pred}= 0.9945			
HHV, SCGs			
Model	9	419.85	<0.0001
X_1	1	4397.56	<0.0001
X_2	1	48.01	<0.0001
X_3	1	50.25	<0.0001
X^2_1	1	8.30	0.007
X^2_2	1	41.40	<0.0001
X^2_3	1	10.65	0.003
X_1X_2	1	33.64	<0.0001
X_1X_3	1	7.63	0.009
X_2X_3	1	17.72	<0.0001
Lack of fit (LOF)	27	1.14	0.478
R^2 = 0.9929, R^2_{adj}= 0.9905, R^2_{pred}= 0.9865			

Table 7

Table 7. Predicted and experimental values of the responses at optimum conditions

Sample	X_1 (°C)	X_2 (min)	X_3 (°C/min)	W_L (%)			HHV (MJ/kg)		
				Measured	Predicted	Deviation (%)	Measured	Predicted	Deviation (%)
CC	271.7	20	5	28.2±0.4	28.7	-1.8	23.15±0.17	23.60	-1.9
SCGs	256.0	20	25	21.9±0.3	21.6	1.4	28.39±0.23	28.18	0.7

Figure 1
Click here to download high resolution image

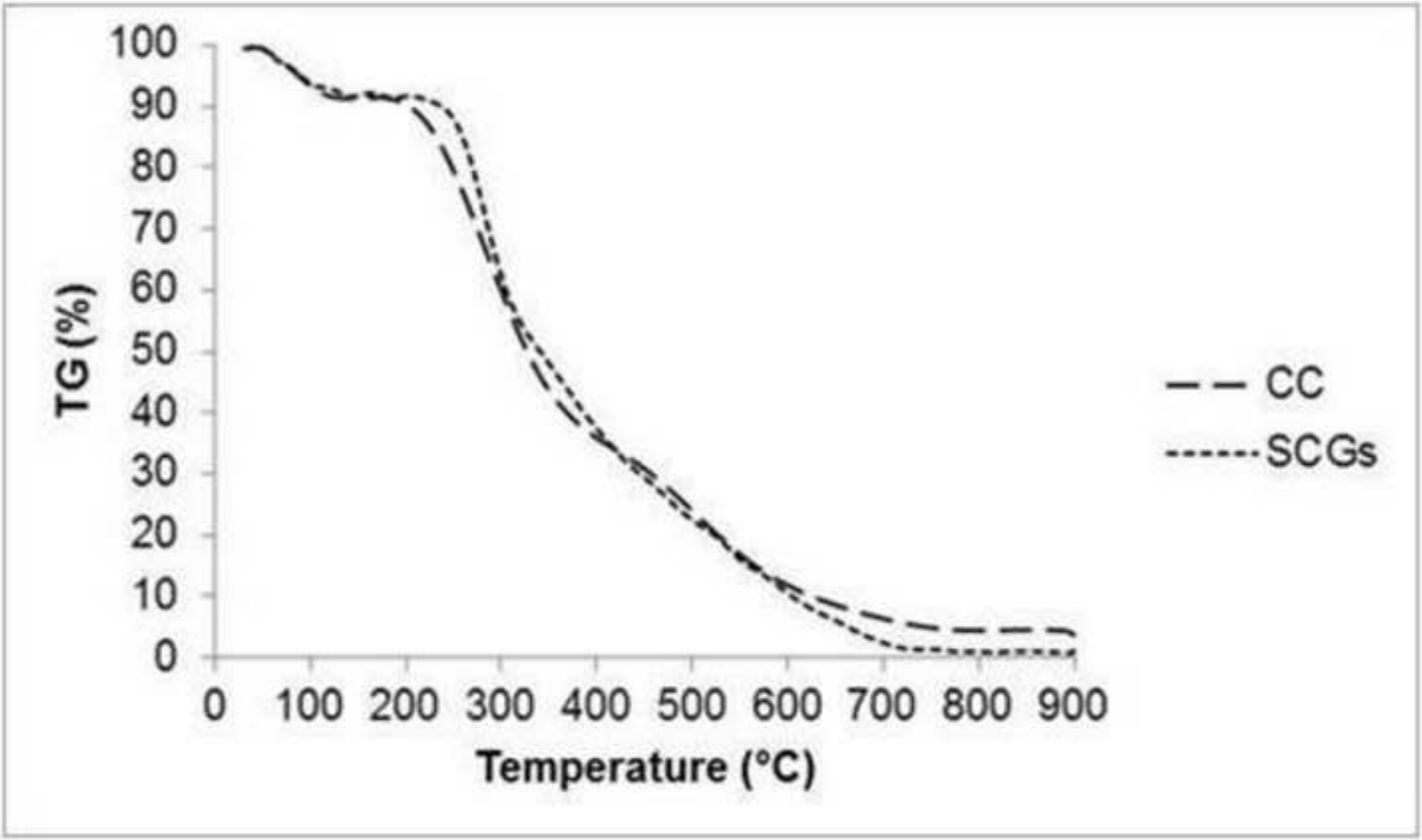

Figure 2
Click here to download high resolution image

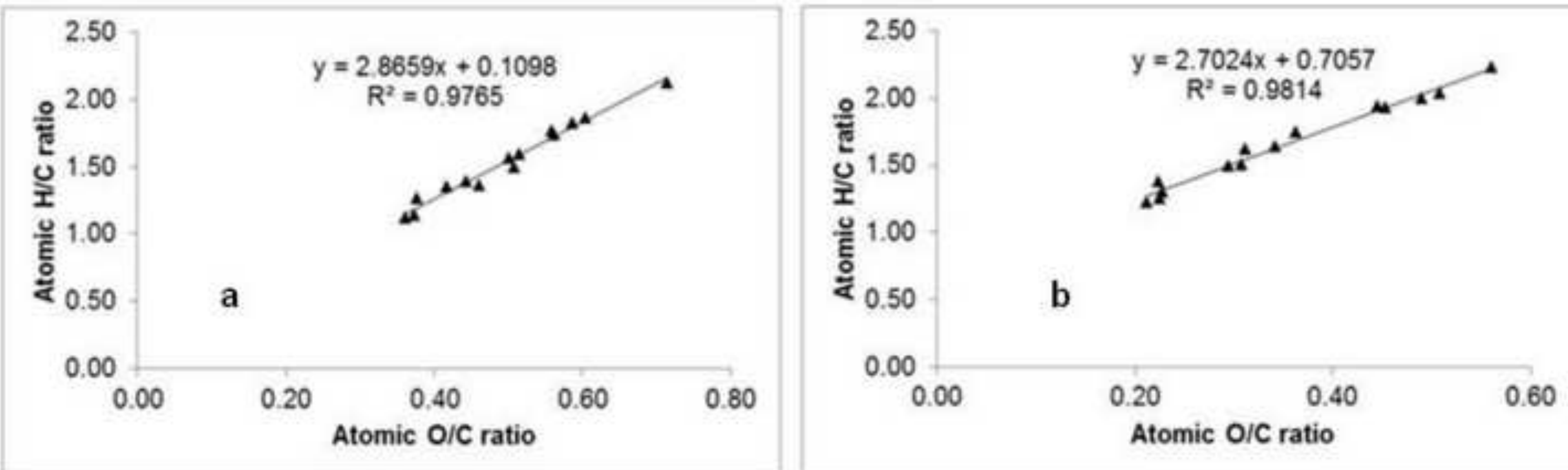

Figure 3
Click here to download high resolution image

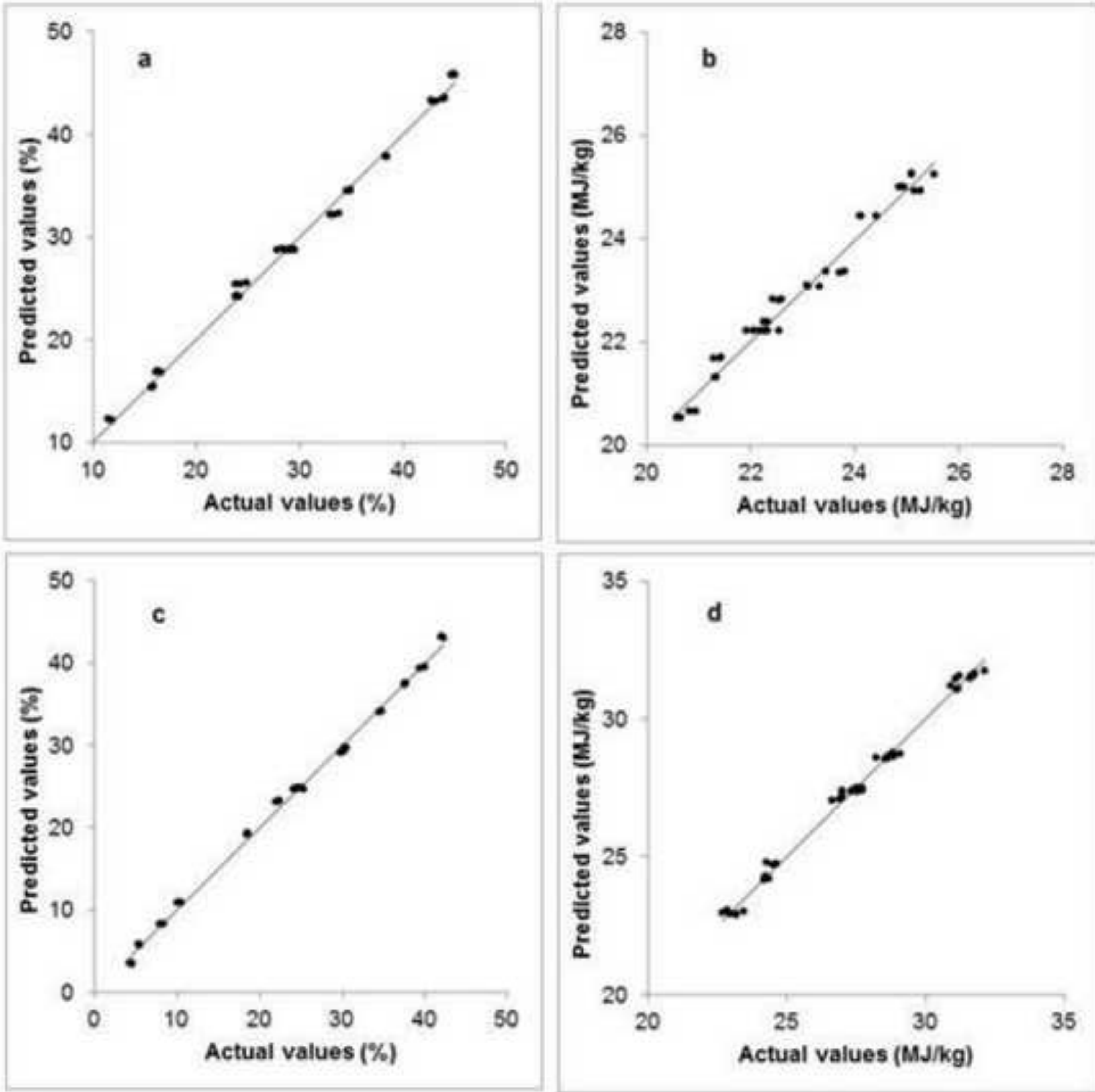

Figure 4
Click here to download high resolution image

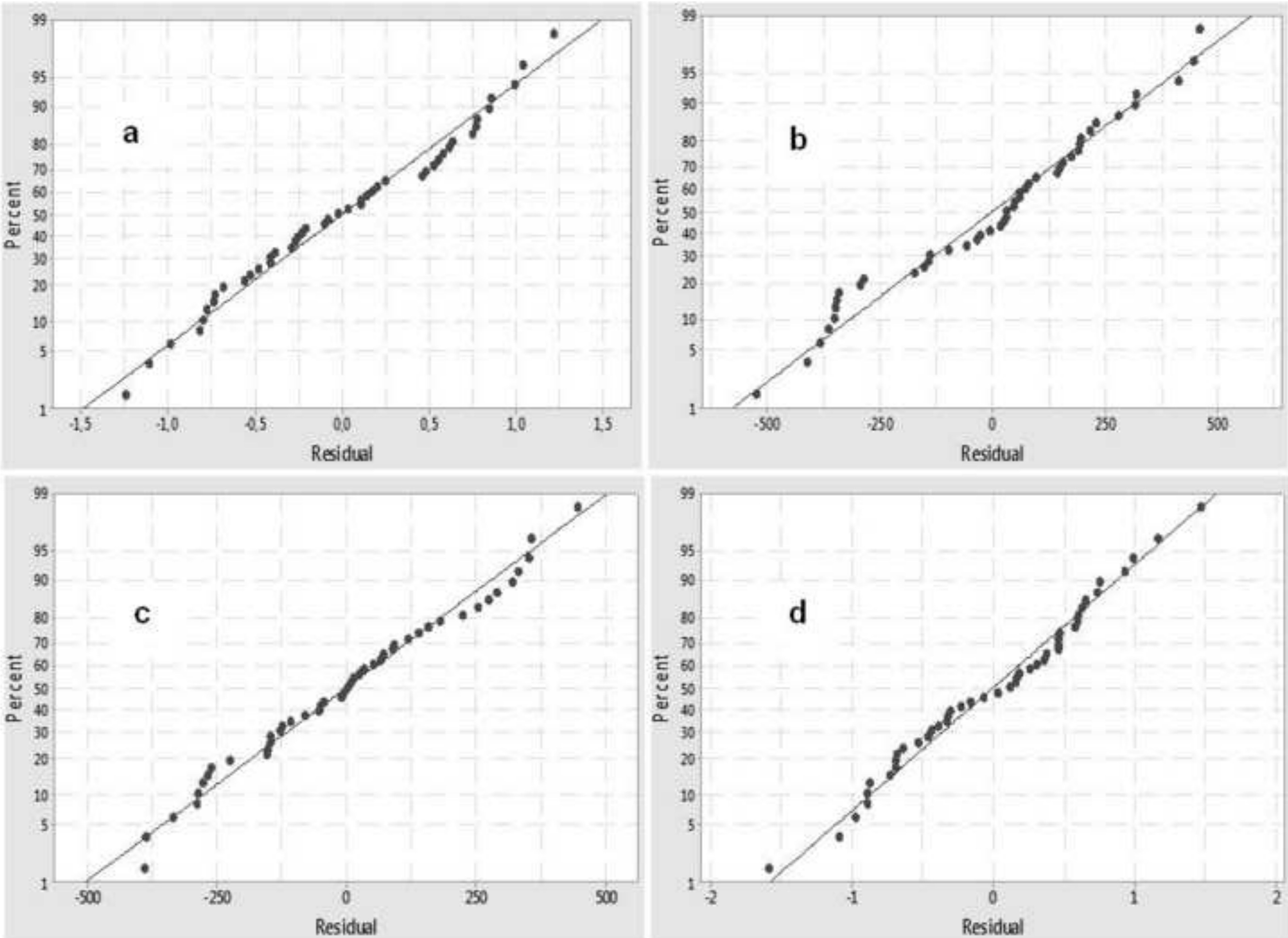

Figure 5

Click here to download high resolution image

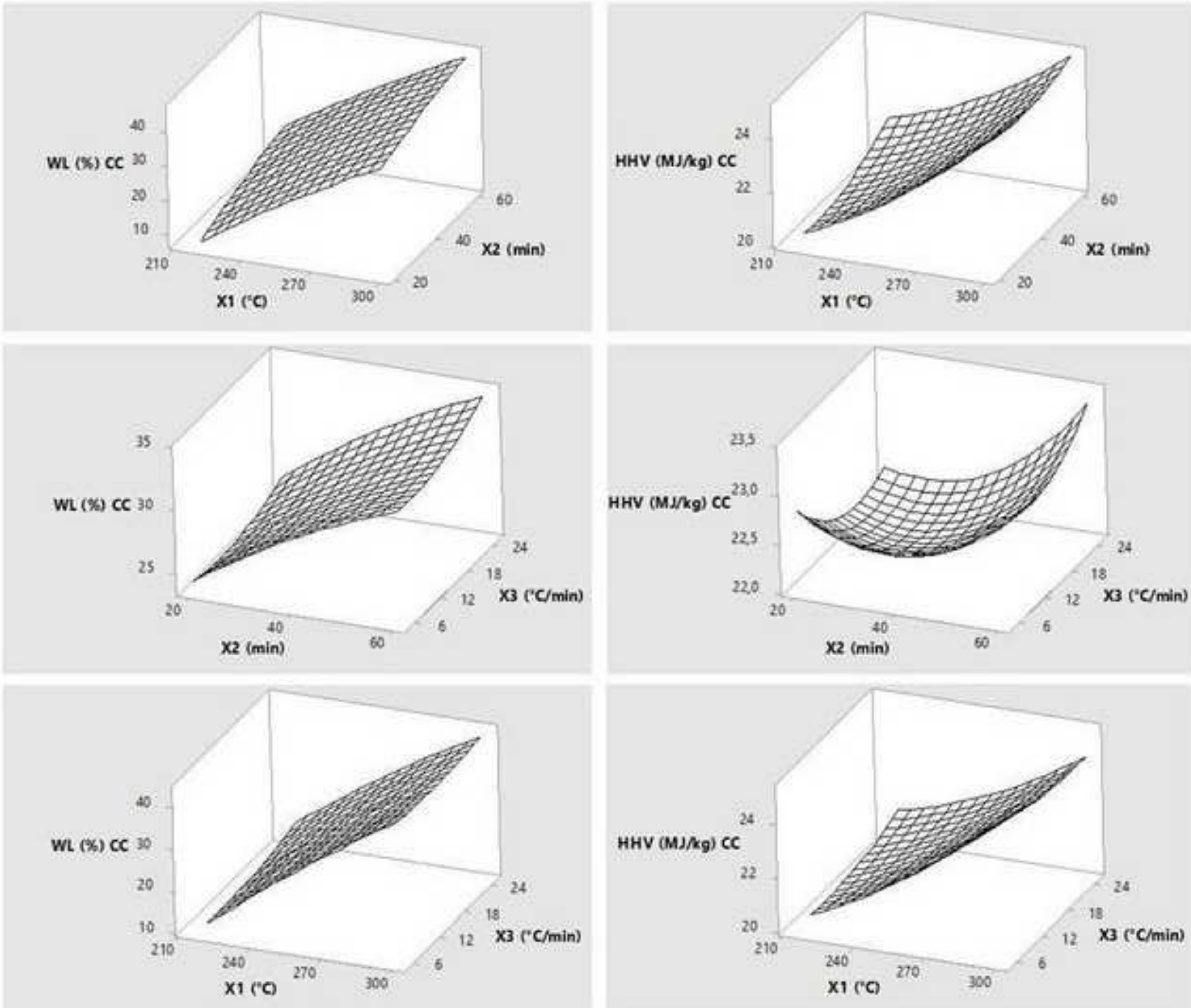

Figure 6
Click here to download high resolution image

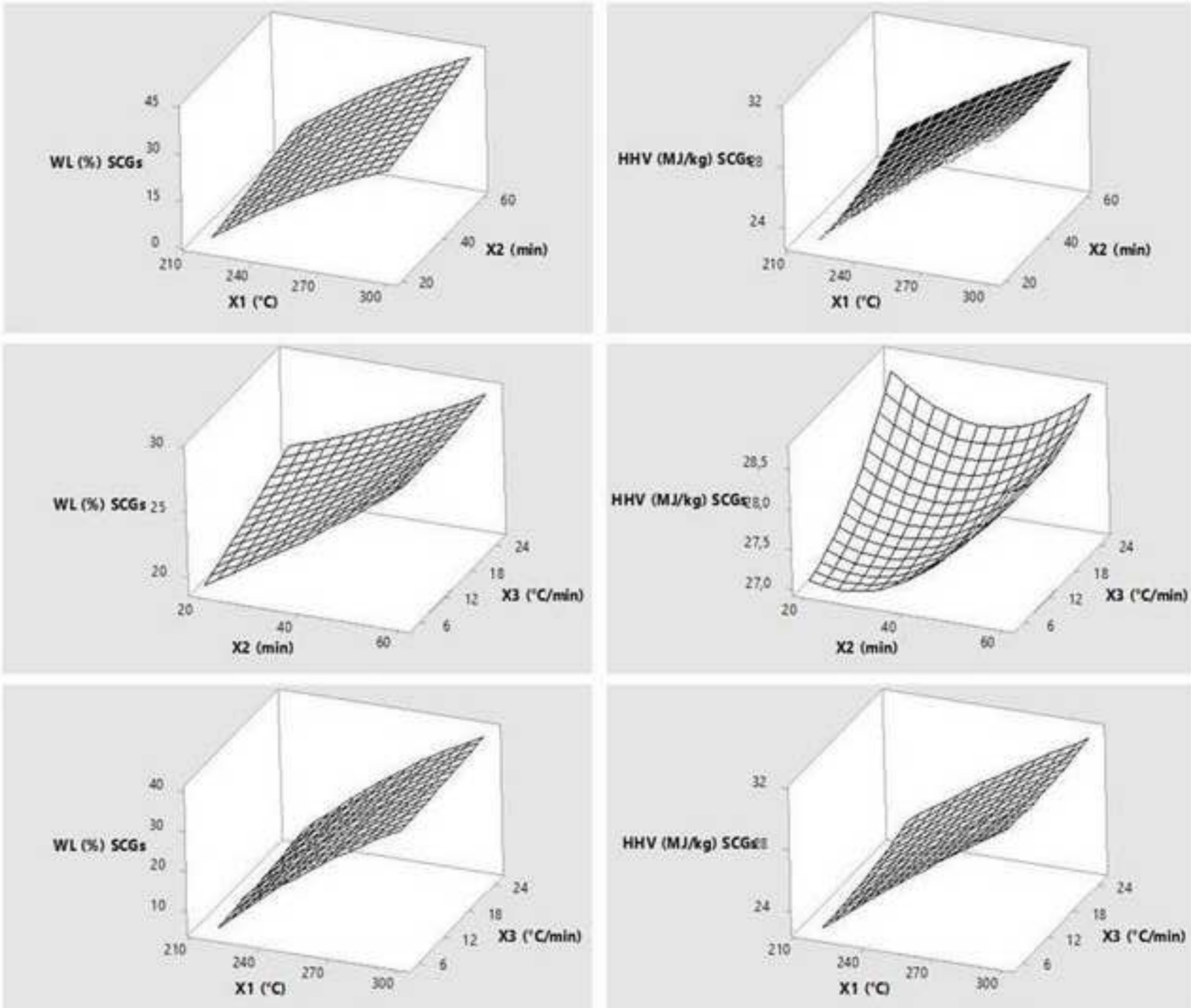

Figure 7

Click here to download high resolution image